Virology 391 (2009) 44–50

Contents lists available at ScienceDirect

Virology

journal homepage: www.elsevier.com/locate/yviro

Portal control of viral prohead expansion and DNA packaging

Krishanu Ray [a,b,1], Mark Oram [a,1], Jinxia Ma [a], Lindsay W. Black [a,*]

[a] Department of Biochemistry and Molecular Biology, University of Maryland School of Medicine, 108 N. Greene St., Baltimore, MD 21201, USA
[b] Center for Fluorescence Spectroscopy, University of Maryland School of Medicine, 725 W. Lombard St., Baltimore, MD 21201, USA

ARTICLE INFO

Article history:
Received 10 February 2009
Returned to author for revision 6 April 2009
Accepted 17 May 2009
Available online 21 June 2009

Keywords:
Bacteriophage
Portal
Terminase
GFP-fusion protein
DNA packaging
Nuclease protection assay
Fluorescence correlation spectroscopy
FCS

ABSTRACT

Bacteriophage T4 terminase packages DNA *in vitro* into empty small or large proheads (esps or elps). *In vivo* maturation of esps yields the more stable and voluminous elps required to contain the 170 kb T4 genome. Functional proheads can be assembled containing portal–GFP fusion proteins. In the absence of terminase activity these accumulated in esps *in vivo*, whereas wild-type portals were found in elps. By nuclease protection assay dsDNAs of lengths 0.1, 0.2, 0.5, 5, 11, 20, 40 or 170 kb were efficiently packaged into wild-type elps *in vitro*, but less so into esps and gp20–GFP elps; particularly with DNAs shorter than 11 kb. However, 0.1 kb substrates were equally efficiently packaged into all types of proheads as judged by fluorescence correlation spectroscopy. These data suggest the portal controls the expansion of the major capsid protein lattice during prohead maturation, and that this expansion is necessary for DNA protection but not for packaging.

Introduction

Most tailed dsDNA bacteriophages package newly replicated DNA into a preassembled empty capsid called the prohead. The phage portal protein plays a key role in all stages of head and mature phage development — both in T4 and other very well characterized model systems. These multi-functional proteins appear highly conserved both in structure and function, and so likely act in a common manner.

Prohead assembly follows a number of pathways among the bacteriophages, but in the case of T4 (and related phages) the procapsid is assembled around a protein core that contributes to assembly and shape determination; the core is then eliminated in part from the procapsid before or during DNA packaging (Black et al., 1994; Showe and Black, 1973). Formation of the bacteriophage T4 prohead has been thoroughly studied from a structural and biochemical perspective and it is known to assemble in a number of discrete stages. Initially the portal protein – a dodecamer of gp20 subunits encoded by T4 gene 20 – becomes attached to the inner surface of the cytoplasmic membrane in an infected host, where it acts as an initiator for the assembly of the core and procapsid structure (Hsiao and Black, 1978; Michaud et al., 1989). The proteinase gp21 component of the core then degrades many of the core proteins and additionally processes most of the assembled procapsid (van Driel et al., 1980). Following proteolytic maturation the "empty" proheads are detached from the membrane, with the portal dodecamer housed at one unique vertex of the icosahedral capsid. The protein also then plays further key roles in the completion of phage morphogeneis, both by acting in concert with the phage terminase enzyme to catalyse DNA packaging (Black, 1989; Lin, Rao, and Black, 1999), and by subsequently binding to a pre-assembled tail structure to complete the assembly of the phage particle (Coombs and Eiserling, 1977; Driedonks and Caldentey, 1983).

Proteolytically processed T4 proheads are observed to fall into two distinct populations, empty small particles, or esps; and empty large particles, or elps (Rao and Black, 1985). Both are composed of the same processed proteins but are structurally distinct, differing in size, volume, stability and charge (Laemmli et al., 1976; Steven et al., 1976). As such, a mix of esps and elps can be readily separated by ion exchange column chromatography (Rao and Black, 1985). Distinct epitopes of the mature (proteolytically processed) capsid protein gp23* are displayed on the exterior of the prohead depending on whether the structure is in the esp or elp form (Kistler et al., 1978; Steven et al., 1991). Additionally, whereas gp23* of the esp is readily dissociated by SDS at room temperature, the capsid proteins of elps are fully resistant to dissociation below 65 °C (Carrascosa, 1978; Carrascosa and Kellenberger, 1978). Packaging of DNA *in vivo* appears to be initiated on esps and DNA packing likely induces the expansion of the esps to elps (Jardine et al., 1998); in fact, only the elp can ultimately contain the full 170 kb T4 genome. However, packaging of DNA into elps *in vitro* has been observed to be substantially more efficient than into esps when this is measured by formation of active phage particles (Rao and Black, 1985) or by protection of packaged

* Corresponding author. Fax: +1 410 706 8297.
E-mail addresses: krishanu@cfs.umbi.umd.edu (K. Ray), moram@umaryland.edu (M. Oram), JMa@som.umaryland.edu (J. Ma), lblack@umaryland.edu (L.W. Black).
[1] These authors contributed equally to the work.

0042-6822/$ – see front matter © 2009 Elsevier Inc. All rights reserved.
doi:10.1016/j.virol.2009.05.029

DNA from nuclease (Black and Peng, 2006). Moreover, expansion from the esp to elp form can also occur in the absence of packaging both *in vivo* and *in vitro* – by low salt dialysis for example – and elps that formed are competent for DNA packaging. The esp to elp transition is thus clearly a key aspect of the overall DNA packaging process.

In previous work designed to probe the mechanism of DNA packaging and define the role of the portal in the process, we constructed T4 proheads that carry fusions of GFP to the C terminus of the gp20 portal subunits (Baumann et al., 2006). Based on known portal structures (Lebedev et al., 2007; Simpson et al., 2000) the C-terminal GFP domain would likely reside immediately within the capsid interior; as confirmed by protease accessibility data (Baumann et al., 2006). Proheads assembled with hetero-oligomeric portal dodecamers, where around half of the subunits were C-terminal GFP fusions and the remainder were near full-length portal subunits, were still fully competent for DNA packaging and phage maturation (Baumann et al., 2006). This result established that substantial structural alterations can be made to the portal dodecamer without significant loss of function. In the current work, by contrast, we now show that the esp to elp expansion is inhibited in proheads containing portal–GFP fusions, thus implicating for the first time prohead expansion as being yet another aspect of phage development that is modulated by the portal itself. We also studied DNA packaging *in vitro* into wild-type or GFP-fusion proheads, in either the esp or elp form. Shorter DNA molecules were apparently poorly translocated into esp proheads as judged by nuclease protection. However, a fluorescence correlation spectroscopy assay, that we recently developed to follow T4 packaging non-invasively (Sabanayagam et al., 2007), revealed efficient DNA packaging into all prohead species examined *in vitro*, suggesting that the expanded elp procapsid is necessary for full nuclease protection of packaged DNA.

Results

Gene 20–GFP fusion protein portals lock proheads in the esp form

Intact but empty proheads accumulate in hosts infected with T4 phages that lack terminase activity, and such infected cultures can be used to prepare purified proheads for packaging assays. Prohead samples from infected, lysed bacteria concentrated by low and high speed centrifugation, followed by 15–45% glycerol gradient centrifugation, contain both esp and elp forms. These in turn can be readily resolved from one another, and from residual nucleic acid contamination by FPLC-DEAE column chromatography (by application of a 0–500 mM NaCl gradient) due to surface charge differences between the esp and elp structures. Fig. 1 shows a typical chromatography profile of a wild-type prohead preparation, from cultures infected at 30 °C. As previously reported (Rao and Black, 1985) the growth temperature of the infected bacterial culture strongly influenced the relative proportion of esps and elps produced. Few esps were routinely produced at 37 °C (not shown) but ~30–50% of the total prohead yield was present as esps at 30 °C (or lower) temperatures (Fig. 1). The separated esp and elp peaks (at 74 and 89 min respectively, corresponding to elution at ~115 nM or ~195 mM NaCl) were readily distinguished by SDS-PAGE. The 45 kDa gp23* of the esps entered the gel upon suspension in SDS buffer at room temperature (Fig. 1 inset, lanes 1 and 2), whereas the same protein of the elps entered the gel only upon heating above 65 °C (lanes 3 and 4).

Proheads containing gp20–GFP (green fluorescent protein fused to the C terminus of portal protein gp20) can be assembled from bacteria that supply the gp20–GFP fusion protein *in trans* from an expression vector, when infected with a T4 mutant lacking the normal portal protein (20*amB8*) as well as the small and large (16*amN66* 17*amA465*)

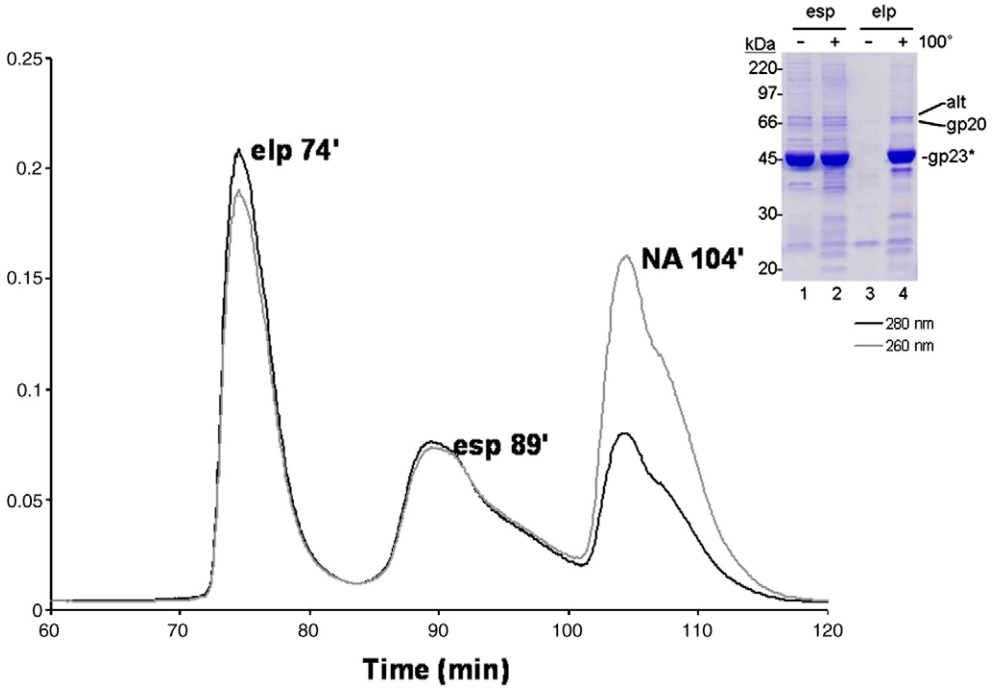

Fig. 1. DEAE chromatography of partially purified normal portal proheads. A mixture of esp and elp proheads was produced by infection at 30 °C of *Escherichia coli* B^E with T4 [13*amE111* 16*amN66* 17*amA465* Δ*rIIA*] phages deficient in terminase and neck protein synthesis. Following concentration and purification of the proheads by low and high speed centrifugation and by 15–45% glycerol gradient centrifugation, the prohead band was resolved by DEAE chromatography by application of a 0–500 mM NaCl gradient (corresponding to 55 to 135 min on the *x* axis). The peaks of elps at 74 min (~115 mM NaCl), esps at 89 min (~195 mM NaCl) and nucleic acid (NA, with the characteristic 2:1 260/280 absorbance profile) at 104 min (~300 mM NaCl) are shown. Inset: Heat stability of the major capsid protein of esp and elp proheads. The solubility of the major capsid protein gp23* from the DEAE peaks of elps (74 min) and esps (89 min) following SDS-PAGE and Coomassie blue staining is shown. Samples were applied to the gel in SDS-sample buffer following (lanes 2 and 4) or without (lanes 1 and3) heating to 100 °C for 4 min. Positions of prohead proteins alt (RNAP modifying injected prohead internal protein), gp20 (portal), and gp23* capsid proteins are indicated.

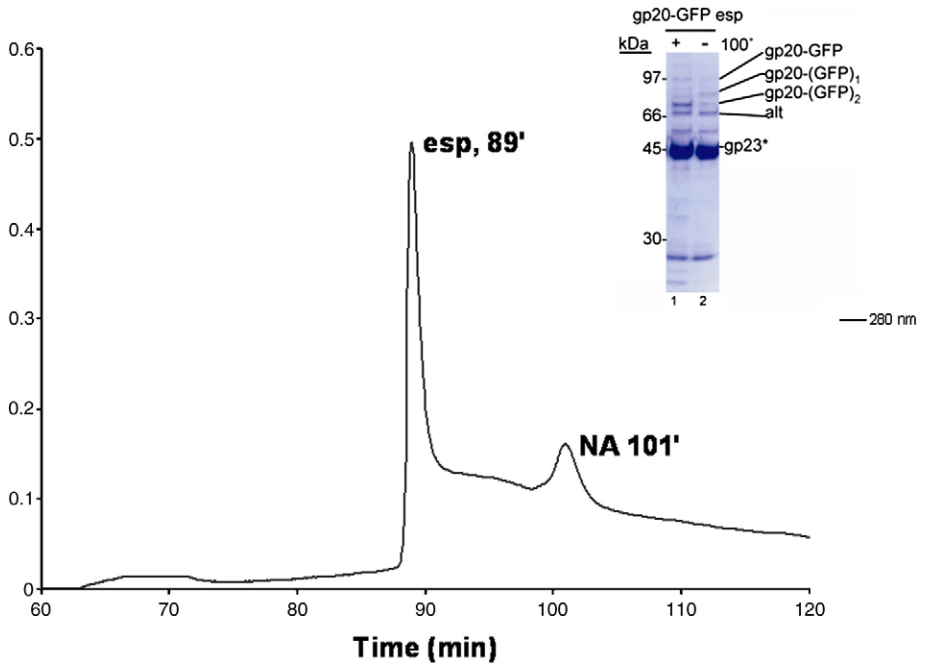

Fig. 2. DEAE chromatography profile of gp20–GFP proheads. A preparation of gp20–GFP containing proheads was obtained from infection of bacteria hosting an induced expression vector (to supply gp20–GFP *in trans*) with a mutant T4 [16*amN66* 17*amA465* 20*amB8 ΔrIIA*] phage stock defective in terminase and gp20 synthesis. Proheads were purified and processed as in Fig. 1. Inset: The gp20–GFP esp peak (~89 min) was applied to the SDS-PAGE with (lane 1) or without heating (lane 2) as in Fig. 1 inset. Positions of relevant prohead portal proteins and gp20–GFP fusions (including truncated species) are on the right of the gels.

gp16 and gp17 terminase subunits (Baumann et al., 2006). Proheads with fusion portal proteins produced in this way typically have about half of the portal subunits tagged with full-length GFP, as judged by Western analysis using GFP and gp20 antibodies. The other portal subunit positions are occupied by gp20–GFP monomers truncated in the GFP domain, or by nearly full-length gp20 monomers — the latter being produced in the infected host since the amber stop codon of the phage 20*amB8* allele is very close to the C terminus of the gene. Co-assembly of fusion-lengthened and truncated monomers is apparently required to form a fully functional portal structure.

In at least half a dozen preparations of gp20–GFP containing proheads produced from bacteria grown at or above 30 °C, only a single peak at the esp position (~85–89 min) was typically observed after DEAE chromatography (Fig. 2). This single peak indeed contained predominantly esps as determined by SDS-PAGE (Fig. 2 inset; lanes 1 and 2). The lack of gp20–GFP proheads in the elp form from such cultures contrasts with preparations of wild-type proheads produced from cultures processed under the same growth conditions and infection temperature (30 °C), where a substantial fraction of elps was routinely observed (Fig. 1). These latter observations also rule out the possibility that failure to mature esps carrying portal gp20–GFP fusions into elps *in vivo* resulted from the growth conditions employed. Instead, this result implicates the gp20–GFP construct itself as being inhibitory to the esp to elp conversion.

Direct genetic and biochemical evidence for the gp20–GFP block to esp maturation was obtained from an experiment that used for infection a strain of the same multiple mutant (16*amN66* 17*amA465* 20*amB8 ΔrIIA H88*) input phage; but one which had accumulated a substantial fraction of 20*amB8* to wild-type revertants or recombinants (between gp20 sequences on the phage and the overexpression plasmid). The DEAE separation profile of proheads in this case (Fig. 3) now showed a minor proportion of elps, as judged by elution in the gradient at 72 min (the normal elp elution position) and resistance of the gp23* to SDS dissociation in the absence of heat (not shown). The major elution peak of esps at 85 and 89 min once again comprised esp proheads. (The small shoulder peak at 89 min likely contained a mix of tailed esps and elps and fully mature phage particles, as indicated by high 260 nm absorption (Rao and Black, 1985). None of these particles were observed from infections using phage that lacked the gp13 neck protein, as with the experiment presented in Fig. 1 for example.) Significantly, a Western blot analysis with a gp20 antibody revealed that the elp peak contained only the normal gp20 protein (Fig. 3 inset, lane 3), exactly as observed with wild-type phage particles (lane 1). The esp peaks (at 85 and 89 min) by contrast now contained gp20–GFP fusion proteins as well as a small amount of the revertant full-length gp20. In addition a substantial amount of the semi-functional 20*amB8* fragment protein was also incorporated (Fig. 3 inset, lanes 4 and 5). Finally, the gp20–GFP esps, but not the wild-type gp20 elps, were highly green fluorescent under UV light (not shown); an observation fully consistent with the Western data. Since only proheads carrying a wild-type portal dodecamer converted to the elp form in a culture carrying mixed forms of portal structures, we conclude that the gp20–GFP fusion protein effectively inhibits the esp to elp conversion.

Despite the block to prohead expansion *in vivo* in the absence of terminase, the portal fusion containing proheads can mature to form viable phage particles when active terminase is present. This was established by the fact that infection of another portion of the same induced culture with the single T4 mutant 20*amB8* yielded ~60 phages per infected bacterium (about half of the typical value for wild-type T4 infections); implying that active DNA packaging can support maturation of the gp20–GFP prohead structure and production of viable phage. Most significantly, upon purification these phages contained precisely the same mixture of portal fusion proteins and long 20*amB8* portal fragment as the esp proheads (Fig. 3 inset, compare lanes 2 and 4); and once again, the gp20–GFP containing phages produced in this fashion were highly green fluorescent. Overall it can be concluded that esp to elp maturation *in vivo* of the gp20–GFP portal containing proheads does occur when terminase activity is available. However in the absence of DNA packaging the gp20–GFP portal proheads are "locked" into the immature esp form, as compared to wild-type portal containing proheads.

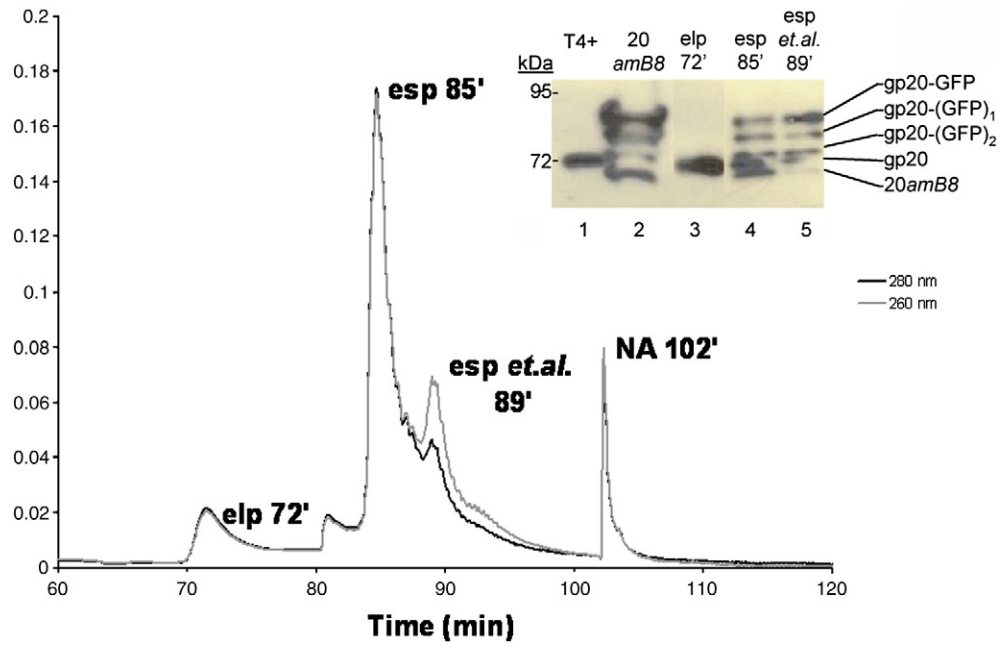

Fig. 3. Western blot analysis of portal forms from purified proheads. A preparation of gp20–GFP containing proheads was obtained from infection of bacteria hosting an induced expression vector (to supply gp20–GFP *in trans*) with a mutant T4 [16*amN66* 17*amA465* 20*amB8* Δ*rIIA*] phage stock that had accumulated significant wild-type gene 20. Proheads were processed as in Fig. 1. Western blots of the elp (72 min) and esp peaks (85 and 89 min) of the peaks from this figure were obtained using an IgY antiserum raised against purified portal protein. Lane 1: purified wild-type T4; lane 2: purified phages produced by a portion of the culture infected with a T4 [20*amB8*] mutant defective only in the portal protein; lane 3: the elp peak (72 min); lanes 4 and 5: the esps peak(s) at 85 and 89 min. Additional tailed proheads or intact phage particles formed at low levels under these conditions and co-eluted at 89 min with the main esp peak; and are shown here as esps et. al. Relevant forms of portal fusions are indicated on the right, molecular weights of marker proteins are in kDa on the left.

Packaging of DNA of varying lengths in vitro into elp and esp forms of wild-type and gp20–GFP proheads

Packaging of linear DNAs into T4 proheads is most efficient when catalysed by the large terminase subunit gp17 in the absence of the small terminase subunit gp16 (Black and Peng, 2006; Kondabagil et al., 2006; Oram et al., 2008). By both nuclease protection and viable phage production assays, DNA packaging *in vitro* into elps was previously observed to be considerably more efficient than into esps (Black and Peng, 2006; Rao and Black, 1985). Likewise, when several preparations of gp20–GFP esp proheads were employed in nuclease protection assays, DNA packaging was barely detectable (data not shown). The esp to elp conversion can be induced *in vitro* by either a low salt dialysis or centrifugation and resuspension into low ionic strength buffer at 4 °C (Carrascosa, 1978; Carrascosa and Kellenberger, 1978). Previously, conversion of esps by dialysis *in vitro* yielded elps that had some packaging activity, as judged by viable phage formation (Rao and Black, 1985), although not the enhanced activity routinely obtained with *in vivo* elps. In this study the gp20–GFP esps were also converted by dialysis into elps, a change confirmed by SDS-PAGE analysis (not shown). However, the converted gp20–GFP elps remained relatively inactive as compared to wild-type elps by the nuclease protection assay, especially when employing shorter DNA substrates (Fig. 4, left panel). A similar profile was obtained with the esps, where less efficient packaging than with elps was observed, but some protection of DNA 11 kb or longer was apparent (Fig. 4, right panel).

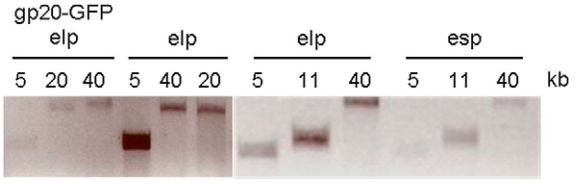

Fig. 4. Efficiencies of proheads in packaging linear DNAs of varying lengths. DNA substrates of varying lengths were used in packaging assays with gp20–GFP elps, wild-type elps (two experiments shown) or esps. After packaging for 60 min, DNase I challenge and then SDS-Proteinase K degradation of the prohead, the samples were analyzed on EtBr-stained agarose gels. DNAs used were pL16 (~5 kb); T7 genomic DNA (40 kb); T7 DNA cut with NheI (yielding 2 fragments ~20 kb in length); pR67 (11 kb), or T3 DNA (40 kb). The lengths of each substrate in kb are given above the lanes.

We also compared the relative packaging efficiencies of elps, esps, and gp20–GFP elps in a more rigorous set of experiments that employed the same numbers of proheads under identical packaging conditions. A range of linear DNA substrates of varying size was used, and the extent of protection from nuclease following packaging was determined by gel densitometry. The wild-type elp proheads packaged short DNAs (0.1, 0.2 or 0.5 kb) highly efficiently, and short DNAs were more efficiently packaged than longer DNAs (Table 1), in line with previous observations (Oram et al., 2008). On the other hand, the esp and gp20–GFP elps appeared markedly less efficient in packaging short DNAs of this size range. Strikingly however, longer DNA molecules were packaged to an appreciable extent by both esp and gp20–GFP elp proheads (Table 1), albeit still with less efficiency than observed with the normal elps.

Packaging in vitro of DNAs by elp, esp, and 20–GFP fusion containing proheads measured by fluorescence correlation spectroscopy

Fluorescence correlation spectroscopy (FCS) is a versatile and powerful technique (Elson, 2001) that can determine the diffusion

Table 1
Relative *in vitro* packaging efficiencies of esp, elp, and gp20–GFP elp proheads employing linear DNAs of different sizes.

DNA size (kb):	0.1	0.2, 0.5	5	11	40	170
gp20–GFP prohead/elp (%)	0	0–4	4	12	15	22
esp/elp (%)	0	0–4	6	30	12	ND
elps: packaged$_{(input)}$	100$_{(100)}$	80$_{(100)}$	11$_{(100)}$	10$_{(100)}$	6$_{(100)}$	6$_{(100)}$

Packaging efficiencies (rows 2 and 3) for each DNA size (columns 2–7) are the % of DNA packaged by each prohead form relative to the amount packaged by elps. The final row shows the percentage of the input DNA packaged into the elp proheads for each DNA size. ND: not determined.

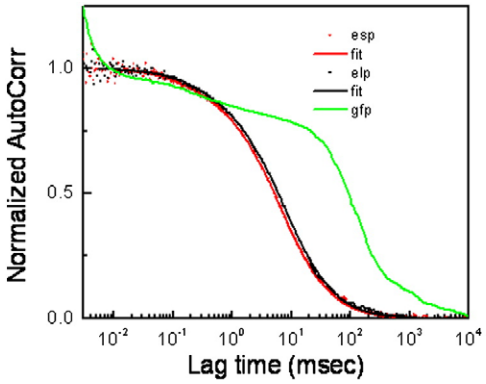

Prohead	Diffusion Coefficients (μm^2/sec)	Contribution (%)
elp	D_1: 3.6	88
	D_2: 114	12
esp	D_1: 4.2	89
	D_2: 120	11
gp20-GFP elp	D_1: 0.24	90

Fig. 5. FCS analysis of packaging into esps, elps and gp20–GFP proheads. Packaging assays were performed with 100 bp Rh-tagged DNA, purified gp17 and purified proheads in varying forms, and incubated in a buffer containing ATP. After 60 min the reactions were analyzed by FCS and the autocorrelation (each normalized to unity) is presented. Data obtained with esp or elp proheads are shown as points, and curves fitted with a two species diffusion model are superimposed as lines. The autocorrelation curve calculated from analysis of packaging assays performed with the gp20–GFP proheads is also shown. The experimental parameters derived from each curve are presented in the accompanying table.

coefficients of fluorescent species (by quantifying the reduction over time of correlations between stochastic fluctuations in the local fluorophore concentration; in a sub-femtolitre volume element in a reaction chamber). An *in vitro* DNA packaging assay we recently developed employs FCS to follow the apparent drop in the diffusion coefficient of short fluorescent DNA substrates as they become encapsidated into the much larger, slower moving proheads (Sabanayagam et al., 2007). In this current work, packaging reactions were set up using esps, elps or gp20–GFP elps with 100 bp rhodamine-tagged DNA substrates, and analyzed by FCS after 60 min. The decay of fluorescence correlation of the 100 bp DNA substrate in a negative control reaction (*i.e.* one lacking proheads: not shown) could be described by a single species diffusion model – implying one fluorescent species present – which yielded a diffusion coefficient of around 125 $\mu m^2/s$ for the free substrate. By contrast, the correlation curves of the reactions using elps (Fig. 5) were best described by a diffusion model incorporating two species, implying that after 60 min two main fluorescing species were now present. The parameters obtained implied that the faster species had a diffusion coefficient of 114 $\mu m^2/s$ with a relative abundance of 12%, while the slower species had a diffusion coefficient of 3.6 $\mu m^2/s$ and a relative abundance of 88%. The diffusion coefficient of the faster species thus corresponded to that of free DNA, while the slower species had a diffusion coefficient approximating that previously calculated for the T4 prohead (Sabanayagam et al., 2007), namely 4.4 $\mu m^2/s$. This analysis thus implied that most (88%) of the input 100 bp DNA is sequestered in the elp prohead after a 60 min packaging reaction. Strikingly, the autocorrelation curve from the reaction with esps was very similar (Fig. 5); and the calculated diffusion coefficients of 4.2 and 120 $\mu m^2/s$ for two species – with relative abundances of 89% and 11% respectively – mirrored very closely the data obtained with elps (Fig. 5). This concordance strongly implied that the esp was as efficient as the elp in packaging 100 bp DNA, as judged by FCS. The gp20–GFP elps appeared to more strongly self-associate, possibly because pelleting and conversion of the esps to elps in low ionic strength buffer led to slower diffusing aggregates. Nevertheless, their packaging ability was largely unimpaired, since analysis of the decay profile implied that 90% or more of the input rhodamine species were sequestered. Overall, the FCS measurements implied that both the esps and gp20–GFP elps were as active as the elps in packaging short DNA molecules, in marked contrast to the data in Table 1 that implied nuclease protection was deficient in these particles as compared to normal elps.

Discussion

Phage DNA packaging is an essential step of the phage life-cycle, is a conserved process amongst a vast number of disparate dsDNA phages, and is the focus of many structural and functional studies. While attention has focused primarily on the mechanism of the terminase packaging enzyme, in this work we have examined the structure and role of the prohead itself in the process. Our data reveal a novel function of the T4 portal – namely that of modulating or initiating the expansion of the esp to the elp form of the prohead – and in addition a combination of *in vitro* assays has highlighted apparent differences between the ability of esps or elps to sequester short linear DNA species.

It was previously determined that about half of the gp20 dodecameric portal positions can be occupied by full-length gp20–GFP fusion proteins. The remaining positions are filled with truncated forms of the fusion protein (truncated in the GFP) or with the long gp20*amB8* fragment; as is consistent with our Western blot results (Fig. 3). Other gene *20 amber* mutations yielding shorter polypeptide fragments (that by themselves are not normally incorporated into the prohead) could also form functional portal dodecamers with the full-length GFP fusion; again with about half the sites carrying the gp20–GFP polypeptide (Baumann et al., 2006). Most likely this ~50% occupancy limit of dodecamer positions by the full-length fusions is due to side-to-side packing constraints, limiting the numbers of extraneous protein domains that can occupy the portal without loss of function. The fact that portal activity was retained even with this substantial additional mass of fusion protein – either embedded together with the DNA inside the head, in the case of the gp20–GFP; or tethered to the procapsid by N-terminal HOC–gp20 fusion protein – strongly suggested that the portal does not operate as a rotary motor (Hendrix, 1978). However these experiments did not rule out an effect of the fusions on other portal functions.

One key finding of this current work, that the T4 gp20–GFP portal blocks esp maturation *in vivo* as compared to wild-type, reveals a new and significant portal function; namely control of procapsid expansion. This function therefore can be added to the list of essential portal phage assembly roles: namely procapsid and core assembly, DNA packaging, DNA cutting, and head to tail joining. The role of the portal in controlling procapsid expansion is entirely consistent with early observations that in a proteolytically processed giant capsid (Steven and Carrascosa, 1979) expansion of the prohead occurs perpendicular to the major axis and in a narrow zone — exactly as would be observed if initiation of the expansion process was portal-driven. Our current observations now strongly suggest that the opening up of the whole procapsid lattice structure (100 nm by 75 nm) is controlled by the relatively small (17 nm by 14 nm) portal (Driedonks et al., 1981) — possibly akin to the function of a small 'runner' acting to expand a much larger umbrella structure for example. The additional mass of GFP fusion domains potentially inhibits this transition, accounting for the gp20–GFP block to elp formation observed in this work.

A model for this process is sketched in Fig. 6. Although a precise structural basis for this proposed activity of the T4 portal is yet to be

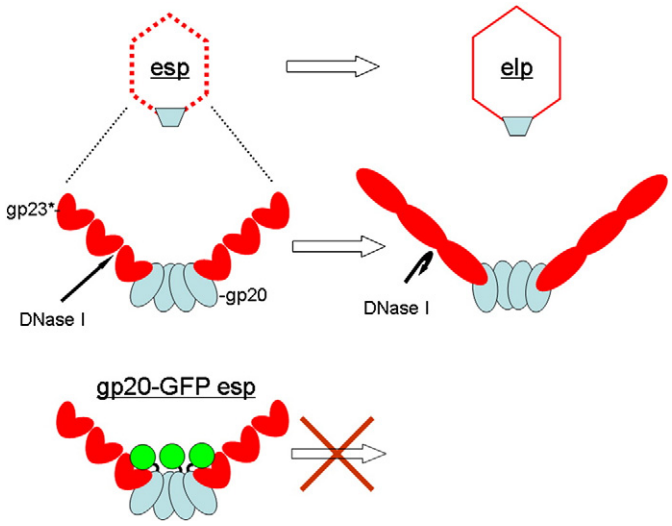

Fig. 6. Role of the portal in prohead expansion and in DNA protection. The esp and elp forms of the T4 prohead are sketched, where the capsid lattice of gp23* subunits is shown in red and the gp20 dodecamer portal in cyan. The central panels show an exploded view of the portal region, where only four of the twelve portal subunits (cyan oval) are shown for clarity. Conversion of esps to elps occurs if the portal initiates the structural changes induced in gp23*; as represented by the altered conformation of the gp20 subunits and the changes in gp23* conformation. The permeability (or otherwise) of the esp or elp lattices to DNase I is sketched by black arrows. With the gp20–GFP C-terminal fusions (with 3 out of 4 subunits shown as fusions in the lower panel) the extra GFP moieties could act to structurally inhibit the esp to elp transition. (For interpretation of the references to colour in this figure legend, the reader is referred to the web version of this article.)

established, conformational changes in the SPP1 portal have been shown to be essential for DNA packaging (Cuervo et al., 2007), and in addition the P22 portal is forced into a distinct conformational state once the head is fully packaged with DNA (Lander et al., 2006). A conformationally versatile structure that can facilitate multiple activities during DNA packaging and phage development may thus be a common aspect of portal function. Our work also implies that portal control of phage T4 prohead expansion is modulated by DNA packaging in both the normal and gp20–GFP portal containing proheads. Although it was previously thought that esp to elp conversion was wholly dependent on DNA packaging, the fact that normal proheads mostly expand *in vivo* in the absence of packaging argues against a simple "DNA pressure" expansion mechanism. Instead, our results favor the alternative that DNA and/or terminase packaging interaction with the portal alters its structure so as to trip the bulk capsid lattice that is poised for the expansion–transformation — again underscoring the central role played by the portal in the expansion process.

Compared to the normal mature elp proheads, the esp and gp20–GFP elp proheads were much less active or virtually packaging inactive on shorter substrates *in vitro* as measured by nuclease protection assay. However a separate FCS assay implied that all the prohead forms examined were equally effective in packaging 100 bp DNA. It is unlikely that the FCS results arose due to DNA being held outside the prohead by the portal, rather than fully packaged; since it was previously shown by FRET that the DNA entered the prohead in proximity to internal protein–GFP fusion proteins prepackaged within the prohead (Sabanayagam et al., 2007). Moreover multiple segments of DNA were packaged per prohead under our experimental conditions (Oram et al., 2008). How then can the divergent results with esps and g20–GFP elp proheads between the nuclease protection and FCS assays be accounted for? The nuclease packaging assay is based on the end-point determination of the amount of DNA protected by a prohead–terminase mixture (following 30–60 min of packaging at room temperature) against DNase I challenge at 37 °C. Formally, it has not been excluded that the nuclease could access the DNA through the immature portal and/or immature procapsid lattice of the esp prohead. Indeed, the T4 prohead scaffold proteins are proteolysed into relatively large peptides; and although a few are retained by the matured DNA-containing capsid the rest mainly exit the esps to provide space for the incoming DNA during packaging (Black et al., 1994). Such a mechanism is also comparable to the exit of large scaffold proteins from procapsids in phages without proteolytic processing (Fu and Prevelige, 2006) and implies that the immature phage prohead lattice is likely permeable to moderately sized proteins. Since DNA inside a normal T4 elp prohead is clearly protected from degradation at 37 °C, the ability (if any) of DNase I to traverse the T4 esp lattice would then be eliminated by the structural changes of the esp to elp transition. The increase in packing efficiency of esps and gp20–GFP proheads that was observed upon increasing the substrate size (Table 1) then suggests that T4 esp expansion might be triggered by packaging between 5 and 11 kb of continuous DNA, providing a nuclease secure container at this point (Fig. 6). It is perhaps noteworthy that the esp to elp transition in phage lambda is triggered by a comparable length of packaged DNA (Fuller et al., 2007; Hohn, 1983). We attempted to demonstrate such a critical size for esp expansion by the SDS-PAGE assay, but these experiments were inconclusive. This result was likely due to insufficient numbers of particles actively translocating DNAs ≥ 11 kb being present at a level that would be needed to demonstrate the packing-dependent conversion of esps to elps under such conditions.

Overall, our experiments suggest that FCS measurement of packaging in real time provides a valuable and possibly more accurate assay of DNA entry into the prohead. They also underscore the potential of fluorescence analysis for analyzing packaging *in vitro*, by demonstrating the activity of portal–GFP proheads with short dye-labeled DNA substrate molecules. Employing such components and assays as presented here will facilitate novel experiments probing the structure and dynamics of the packaging motor.

Materials and methods

Prohead purification and analysis

Preparation of wild-type esps and elps by infection with T4 [13*amE111* 16*amN66* 17*amA465* Δ*rIIA H88*] phages deficient in terminase (genes 16 and 17) and neck (gene 13) protein synthesis followed procedures previously described (Black and Peng, 2006; Rao and Black, 1985); the rII mutation allows assay of phage assembly following packaging of mature T4 DNA. Following purification by centrifugation and glycerol gradient ultracentrifugation, the final prohead purification step, FPLC-DEAE chromatography, employed a linear 0–500 mM NaCl salt gradient starting at 55 min, and peaks are identified by the elution time. Preparations of gp20–GFP containing proheads (Baumann et al., 2006) followed the same protocol; employing a mutant T4 [16*amN66* 17*amA465* 20*amB8* Δ*rIIA H88*] phage defective in terminase and portal protein synthesis grown on a host also containing a gp20–GFP expression plasmid. Presence of GFP fusion particles was confirmed by visible induced green fluorescence upon UV exposure, as well as by SDS-PAGE. Western analysis of prohead-containing column fractions employed a chicken IgY antibody raised to the T4 gp20 portal protein (Baumann et al., 2006) and followed standard protocols (Sambrook et al., 1989). Prohead concentrations for packaging assays were quantified by OD_{280} absorption and relative gp23* SDS-PAGE band intensity in relation to known active phage T4 particle concentrations.

Packaging assays

DNA substrates for nuclease packaging assays comprised purified plasmids or phage T3, T4 or T7 DNAs purified, linearized and

shortened by standard means (Sambrook et al., 1989). 100 bp Rh-tagged molecules were prepared as described (Sabanayagam et al., 2007). Nuclease protection and FCS assays of packaging comparing equal numbers of esp, elp, and gp20–GFP elp proheads were as described previously (Black and Peng, 2006). FCS measurements were performed using a Picoquant MicroTime 200 confocal microscope (Picoquant microtime system coupled to an Olympus IX71 microscope). The excitation laser (λ_{ex}~470 nm) was reflected by a dichroic mirror to a high numerical aperture (NA) oil objective (100×, NA 1.3) and focused onto the solution sample. The fluorescence was collected by avalanche photodiodes through a dichroic beam splitter and longpass (Chroma) filter thus eliminating the scattered excitation light and collecting the fluorescence from the rhodamine probes in the region of interest. PicoQuant Symphotime software (version 4.3) was used to generate the autocorrelation curves; these in turn were fitted to the pure diffusion model described (Sabanayagam et al., 2007).

Acknowledgments

We thank the staff at the University of Maryland Center for Fluorescence Studies for support and for access to equipment. This work was supported by NIH grant AI11676.

References

Baumann, R.G., Mullaney, J., Black, L.W., 2006. Portal fusion protein constraints on function in DNA packaging of bacteriophage T4. Mol. Microbiol. 61 (1), 16–32.
Black, L.W., 1989. DNA packaging in dsDNA bacteriophages. Annu. Rev. Microbiol. 43, 267–292.
Black, L.W., Peng, G., 2006. Mechanistic coupling of bacteriophage T4 DNA packaging to components of the replication-dependent late transcription machinery. J. Biol. Chem. 281 (35), 25635–25643.
Black, L.W., Showe, M.K., Steven, A.C., 1994. Morphogenesis of the T4 Head. In: Karam, J.D. (Ed.), Molecular Biology of Bacteriophage T4. InAmerican Society for Microbiology, Washington DC, pp. 218–258.
Carrascosa, J.L., 1978. Head maturation pathway of bacteriophages T4 and T2. IV. In vitro transformation of T4 head-related particles produced by mutants in gene 17 to capsid-like structures. J. Virol. 26 (2), 420–428.
Carrascosa, J.L., Kellenberger, E., 1978. Head maturation pathway of bacteriophages T4 and T2. III. Isolation and characterization of particles produced by mutants in gene 17. J. Virol. 25 (3), 831–844.
Coombs, D.H., Eiserling, F.A., 1977. Studies on the structure, protein composition and assembly of the neck of bacteriophage T4. J. Mol. Biol. 116 (3), 375–405.
Cuervo, A., Vaney, M.C., Antson, A.A., Tavares, P., Oliveira, L., 2007. Structural rearrangements between portal protein subunits are essential for viral DNA translocation. J. Biol. Chem. 282 (26), 18907–18913.
Driedonks, R.A., Caldentey, J., 1983. Gene 20 product of bacteriophage T4. II. Its structural organization in prehead and bacteriophage. J. Mol. Biol. 166 (3), 341–360.
Driedonks, R.A., Engel, A., tenHeggeler, B., van Driel, R., 1981. Gene 20 product of bacteriophage T4 its purification and structure. J. Mol. Biol. 152 (4), 641–662.
Elson, E.L., 2001. Fluorescence correlation spectroscopy measures molecular transport in cells. Traffic 2 (11), 789–796.
Fu, C.Y., Prevelige Jr, P.E., 2006. Dynamic motions of free and bound Φ29 scaffolding protein identified by hydrogen deuterium exchange mass spectrometry. Protein Sci. 15 (4), 731–743.
Fuller, D.N., Raymer, D.M., Rickgauer, J.P., Robertson, R.M., Catalano, C.E., Anderson, D.L., Grimes, S., Smith, D.E., 2007. Measurements of single DNA molecule packaging dynamics in bacteriophage lambda reveal high forces, high motor processivity, and capsid transformations. J. Mol. Biol. 373 (5), 1113–1122.
Hendrix, R.W., 1978. Symmetry mismatch and DNA packaging in large bacteriophages. Proc. Natl. Acad. Sci. U. S. A. 75 (10), 4779–4783.
Hohn, B., 1983. DNA sequences necessary for packaging of bacteriophage lambda DNA. Proc. Natl. Acad. Sci. U. S. A. 80 (24), 7456–7460.
Hsiao, C.L., Black, L.W., 1978. Head morphogenesis of bacteriophage T4. II. The role of gene 40 in initiating prehead assembly. Virology 91 (1), 15–25.
Jardine, P.J., McCormick, M.C., Lutze-Wallace, C., Coombs, D.H., 1998. The bacteriophage T4 DNA packaging apparatus targets the unexpanded prohead. J. Mol. Biol. 284 (3), 647–659.
Kistler, J., Aebi, U., Onorato, L., ten Heggeler, B., Showe, M.K., 1978. Structural changes during the transformation of bacteriophage T4 polyheads: characterization of the initial and final states by freeze-drying and shadowing Fab-fragment-labelled preparations. J. Mol. Biol. 126 (3), 571–589.
Kondabagil, K.R., Zhang, Z., Rao, V.B., 2006. The DNA translocating ATPase of bacteriophage T4 packaging motor. J. Mol. Biol. 363 (4), 786–799.
Laemmli, U.K., Amos, L.A., Klug, A., 1976. Correlation between structural transformation and cleavage of the major head protein of T4 bacteriophage. Cell 7 (2), 191–203.
Lander, G.C., Tang, L., Casjens, S.R., Gilcrease, E.B., Prevelige, P., Poliakov, A., Potter, C.S., Carragher, B., Johnson, J.E., 2006. The structure of an infectious P22 virion shows the signal for headful DNA packaging. Science 312 (5781), 1791–1795.
Lebedev, A.A., Krause, M.H., Isidro, A.L., Vagin, A.A., Orlova, E.V., Turner, J., Dodson, E.J., Tavares, P., Antson, A.A., 2007. Structural framework for DNA translocation via the viral portal protein. EMBO J. 26 (7), 1984–1994.
Lin, H., Rao, V.B., Black, L.W., 1999. Analysis of capsid portal protein and terminase functional domains: interaction sites required for DNA packaging in bacteriophage T4. J. Mol. Biol. 289 (2), 249–260.
Michaud, G., Zachary, A., Rao, V.B., Black, L.W., 1989. Membrane-associated assembly of a phage T4 DNA entrance vertex structure studied with expression vectors. J. Mol. Biol. 209 (4), 667–681.
Oram, M., Sabanayagam, C., Black, L.W., 2008. Modulation of the packaging reaction of bacteriophage T4 terminase by DNA structure. J. Mol. Biol. 381 (1), 61–72.
Rao, V.B., Black, L.W., 1985. DNA packaging of bacteriophage T4 proheads in vitro. Evidence that prohead expansion is not coupled to DNA packaging. J. Mol. Biol. 185 (3), 565–578.
Sabanayagam, C.R., Oram, M., Lakowicz, J.R., Black, L.W., 2007. Viral DNA packaging studied by fluorescence correlation spectroscopy. Biophys. J. 93 (4), L17–L19.
Sambrook, J., Fritsch, E.F., Maniatis, T., 1989. Molecular Cloning: A Laboratory Manual, 2nd Edition. Cold Spring Harbor Laboratory Press, Cold Spring Harbor, New York, p. 11724.
Showe, M.K., Black, L.W., 1973. Assembly core of bacteriophage T4: an intermediate in head formation. Nat. New Biol. 242 (116), 70–75.
Simpson, A.A., Tao, Y., Leiman, P.G., Badasso, M.O., He, Y., Jardine, P.J., Olson, N.H., Morais, M.C., Grimes, S., Anderson, D.L., Baker, T.S., Rossmann, M.G., 2000. Structure of the bacteriophage phi29 DNA packaging motor. Nature 408 (6813), 745–750.
Steven, A.C., Carrascosa, J.L., 1979. Proteolytic cleavage and structural transformation: their relationship in bacteriophage T4 capsid maturation. J. Supramol. Struct. 10 (1), 1–11.
Steven, A.C., Couture, E., Aebi, U., Showe, M.K., 1976. Structure of T4 polyheads. II. A pathway of polyhead transformation as a model for T4 capsid maturation. J. Mol. Biol. 106 (1), 187–221.
Steven, A.C., Bauer, A.C., Bisher, M.E., Robey, F.A., Black, L.W., 1991. The maturation-dependent conformational change of phage T4 capsid involves the translocation of specific epitopes between the inner and the outer capsid surfaces. J. Struct. Biol. 106 (3), 221–236.
van Driel, R., Traub, F., Showe, M.K., 1980. Probable localization of the bacteriophage T4 prehead proteinase zymogen in the center of the prehead core. J. Virol. 36 (1), 220–223.